ELSEVIER

Journal of Nuclear Materials 313–316 (2003) 370–376

journal of nuclear materials

www.elsevier.com/locate/jnucmat

Analyses of erosion and re-deposition layers on graphite tiles used in the W-shaped divertor region of JT-60U

Y. Gotoh [a,*], J. Yagyu [a], K. Masaki [a], K. Kizu [a], A. Kaminaga [a], K. Kodama [a], T. Arai [a], T. Tanabe [b], N. Miya [a]

[a] *Naka Fusion Research Establishment, Japan Atomic Energy Research Institute, 801-1, naka-machi, Naka-gun, Ibaraki-ken 311-01, Japan*

[b] *Center for Integrated Research in Science and Engineering, Nagoya University, Japan*

Abstract

Erosion and re-deposition profiles were studied on graphite tiles used in the W-shaped divertor of JT-60U in June 1997–October 1998 periods, operated with all-carbon walls with boronizations and inner-private flux pumping. Continuous re-deposition layers were found neither on the dome top nor on the outer wing, while re-deposition layers of around 20 μm thickness were found on the inner wing, in the region close to the dome top. On the outer divertor target, erosion was found to be dominant: maximum erosion depth of around 20 μm was measured, while on the inner target, re-deposition was dominant: columnar structure layers of maximum thickness at around 30 μm on the inner zone while laminar/columnar-layered structures of maximum thickness around 60 μm were found on the outer zone. Poloidal distributions of the erosion depth/re-deposition layer thickness were well correlated with the frequency histograms of strike point position, which were weighted with total power of neutral beam injection, on both the outer and inner targets. Through X-ray photoelectron spectroscopy, composition of the re-deposition layers at a mid zone on the inner target were 3–4 at.% B and <0.6 at.% O, Fe, Cr, and Ni with remaining C. Boron atoms are mostly bound to C atoms but some may precipitated as boron.

PACS: 52.40.H
Keywords: Plasma-wall interactions; Divertor; Erosion; Re-deposition; Carbon; Boron

1. Introduction

Studies on erosion/re-deposition on the walls of fusion experimental devices are indispensable for elucidation and controls of both (1) impurity generation, transport and accumulation processes, and (2) hydrogen isotope behaviors and their long-term inventories in the vacuum vessel, as well as for (3) lifetime estimation of divertor target plates. Recently, more increasing efforts have been devoted in those fields [1–3].

From late 2000, systematic analysis studies of graphite armor tiles from JT-60U in D–D discharge experimental periods have been started: Studies through scanning electron microscopy (SEM), X-ray photoelectron spectroscopy (XPS) [4], secondary ion mass spectrometry [4], liquid scintillation counting method [5] and imaging plate method for 3H analyses [6] have been made.

In the present study, erosion and re-deposition, as well as atomic compositions of re-deposited layers were investigated for armor tiles used in divertor regions of JT-60U just after the W-shaped divertor modification in 1997. Erosion depths were directly measured through

* Corresponding author. Tel.: +81-29 270 7434; fax: +81-29 270 7449.
E-mail address: gotohy@dai2mc.naka.jaeri.go.jp (Y. Gotoh).

0022-3115/03/$ - see front matter
PII: S0022-3115(02)01354-5

surface profilometry by using a dial gauge. Re-deposition layer thickness and their microstructures were analyzed (SEM) at sectioned specimens, while composition/chemical states of re-deposition layers were analyzed through XPS.

2. Experimental procedures

Fig. 1 shows poloidal locations of analyzed tiles in the W-shaped divertor region of JT-60U. A poloidal set of inner and outer divertor target tiles (5DV2aq, 2bq, 2cq, and 2dq), a dome top tile (5DM2bq), and inner and outer wing tiles (5DM2aq, 2cq), were sampled from #P5 section in Dec. 1998. In the operation periods, June 1997–October 1998, about 4300 discharge (3600 D–D discharge) experiments were made with W-shaped divertor configurations with (or without) inner-private flux pumping through a full toroidal inner slot. More than 300 shots accompanied neutral beam injection (NBI) with the highest power in the 14–23 MW range. Two times of boronization (with 70 g then 50 g of $B_{10}H_{14}$) were conducted in July 1997 and in March 1998.

The net erosion depths on the tiles were estimated from difference between effective tile-thickness changes due to both erosion and re-deposition (surface profilometry: dial gauge), and deposited layer thickness (SEM). The precision of the dial gauge measurements was estimated at around 3 μm through measurements of poloidal total-thickness distribution for as-fabricated target tiles. Both poloidal distributions in the thickness of, and the sub-μm structures of the re-deposition layers were investigated (SEM: Hitachi type S-300H). Vertically sectioned faces of re-deposited layers on the tiles were prepared by fracturing the tiles in the poloidal direction at slit notches of a 0.5 mm width, formed at the rear face, along the toroidal center of the tiles. Observations were made at a beam voltage as low as 4.91 kV. Thus, re-deposited layer thickness as small as 0.2 μm was observed. Elemental and chemical state analyses were made on the re-deposited layers of a thickness around 5 μm by using XPS (ULVAC-PHI: type 5600, MgK_α X-ray source). For depth analyses, sputtering rate for graphite was estimated at around 0.04 nm/s for argon ion sputter-etching at a beam voltage of 4 kV, a beam current, 13.8 nA and a luster-area of 3 mm × 3 mm.

3. Results and discussion

3.1. Microstructure observations

Fig. 2(a)–(d) show poloidal sectional SEM images of top surface layers on graphite tiles: (a) inner dome wing (isotropic graphite: IG-430U), (b) dome top (CFC: PCC-2S), (c) outer dome wing (IG-430U), and (d) 5DV2cq tile of the outer divertor target (CX-2002U). In the dome region, nearly 20-μm-thick re-deposition layers were observed on the inner wing at least in the zone close to the dome top, whereas continuous re-deposition layers were not found on the dome top nor on the outer wing. On the outer divertor target, almost no re-deposition layers were observed by using SEM at front faces as shown in Fig. 2(d) (except in the limited area adjacent to hole-edges). In the heavily eroded areas, somewhat wavy structure surfaces were observed. Maximum erosion depth was measured at around 20 μm (Fig. 6(a)). Fig. 3(a) and (b) show poloidal sectional images of re-deposition layers on 5DV2aq tile (a), and 5DV2bq tile (b) of the inner divertor target. Right-hand side images are enlarged ones from square areas on the left images. In the right-hand images, columnar structure layers on the 5DV2aq tile (Fig. 3(a)), while dense and lamellar over-layers (nearly 30 μm thick) on porous columnar layers (nearly 30 μm), totally of 60 μm thickness, are observed in the maximum re-deposition zone on the 5DV2bq (Figs. 3(b) and 7(a)). From those results,

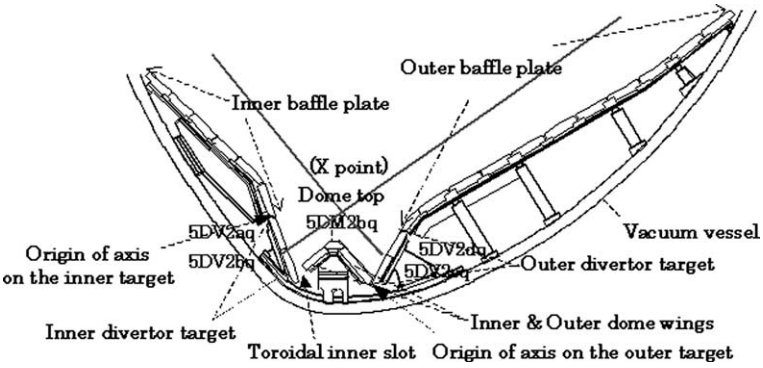

Fig. 1. Poloidal positions of CFC and graphite tiles from divertor targets, dome top and dome wings in the W-shaped divertor region of JT-60U in July 1997–October 1998 periods.

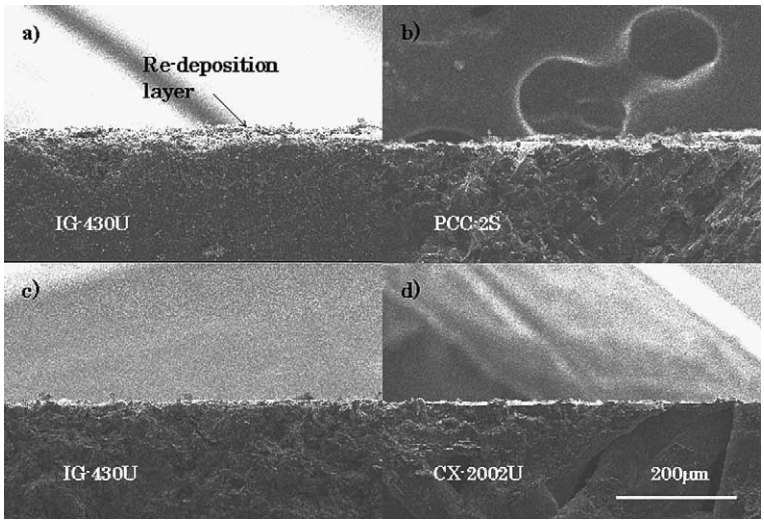

Fig. 2. Cross-sectional SEM images taken at top surface layers on the tiles of the inner dome wing (a), the dome top (b), the outer dome wing (c), and on the tile 5DV2cq of the outer divertor target (d).

volumetric densities of the porous columnar layers of the re-deposited layers seem to be lower than that of the substrate graphite. Columnar structures were sometimes observed to be oriented at around 60° to the tile front faces in a poloidal plane (Fig. 3(a)), which is very close to the poloidal angle at around 65° of the magnetic field line to the target front face. Although toroidal angles of the columnar structures were observed to be about 10 times larger than those at 1.5°–3° of the magnetic field line, the close correlations found for the angles in the poloidal plane might be indications for the existence of some effect of the magnetic field on the re-deposition processes.

The columnar structures were observed for all of the re-deposition layers on the inner target, while the lamellar structures were only observed at the shallower depths in the thicker layers, as lamellar/columnar-layered structures. Therefore, those lamellar structures can be speculated to be due to the higher deposition temperatures when the thicker layers with underneath columnar layers, possibly of the lower thermal conductivity, were positioned under the higher heat fluxes in the strike point zone. At higher temperatures, re-deposition layers may become more graphitic because of the higher probability in C–D bond breaking and the higher mobility of carbon atoms on the surface. As is shown in Section 3.2, coexistence of boron in the deposited layers may also enhance graphitization of the deposited layers.

3.2. Compositional analyses of the re-deposited layers

Fig. 4 shows XPS depth analysis results, with insertion of a cross-sectional SEM image of the re-deposition layer on the inner divertor target at 110 mm from the target inboard end, where the re-deposition layers were the thinnest, at around 5 μm (Fig. 7(a)). In the re-deposition layer, other than main constituent of C, 3–4 at.% B and 0.3–0.6 at.% O, Fe, Ni, Cr were detected. The intensity of boron showed a maximum at around 3 μm depth, possibly corresponding to the first boronization in the periods. Fig. 5 shows a series of B-1s spectra at different depths in the re-deposition layer on the tile. From the results that oxygen concentration in the re-deposition layers is low (Fig. 4) and the present B-1s lines are centered at around 188.8 eV, most of boron atoms are concluded to be not forming B–O_x, but very probably B–C bonds, and possibly some atoms are in B–B bonds.

3.3. Poloidal distributions of erosion/re-deposition

Fig. 6(a)–(c) compare poloidal distributions of erosion depths (a) and the frequency histograms of strike point position on the outer target in the poloidal direction during the experimental periods (b) and that with weight of total NBI power for each shot, $P_{\langle NB \rangle}$, (c) in order the effects of NBI power deposition profile on the erosion to be estimated. Strike point positions were estimated for the vacuum vessel kept at baking temperature of 573 K. Fig. 7(a)–(c) show results for the inner targets. Horizontal axes in Figs. 6 and 7 are determined to be parallel to the target front faces in the poloidal plane, with the origins at the innermost inboard ends of the target plates (Fig. 1). In Figs. 6(a) and 7(a), estimated erosion depth (open squares) was determined from difference between effective tile-thickness changes caused by erosion/re-deposition measured by dial gauge

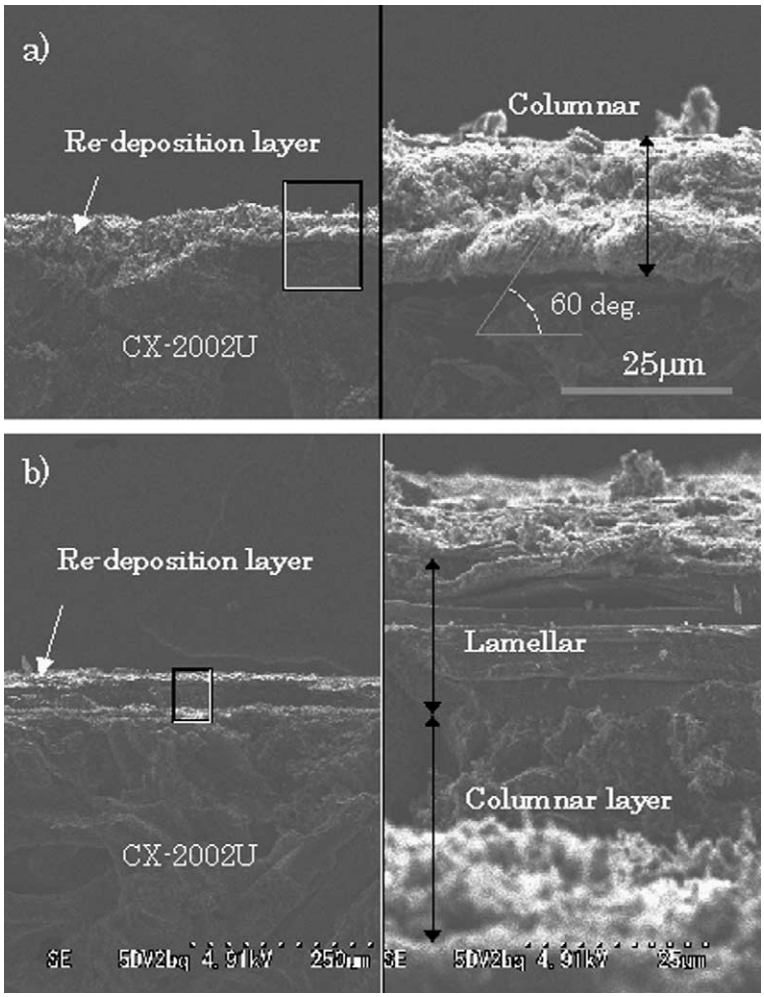

Fig. 3. Cross-sectional SEM images of re-deposition layers on the inner divertor target tiles. Right images are magnified images of enclosed areas in the left images. (a) Columnar structure layers at 65 mm, (b) lamellar/columnar-layered structures at 160 mm from the inboard end of the inner target shown in Fig. 7.

(open triangles) and re-deposition layer thickness from SEM observations (open circles). In Figs. 6(b) and 7(b), as the strike point position may vary during a shot, the distributions of the strike point positions at 4.5, 7.5 and 11.5 s were compared, showing almost similar profiles in a zone ranging 25–170 mm on the outer, while in a zone 20–230 mm on the inner target, respectively. In Fig. 6, the major erosion zone centered at around 90 mm shifted slightly outboard compared with peak position of the histogram of the strike point position on the outer target at around 70–80 mm, while the major deposition zone centered at around 160 mm on the inner target rather correlates well with that around 160 mm (Fig. 7). The full poloidal width of the erosion zone of around 120 mm on the outer target and that of the re-deposition zone of around 210 mm on the inner target are much wider than the widths of particle flux distributions at the strike point possibly around 20–50 mm [7]. Therefore, the observed major structures in the erosion/re-deposition distributions can be correlated with the histograms of the strike point position modified with effective widths of the particle or power flux profiles. The observed outboard shift of the erosion zone compared with the major peak in the strike point distribution may be due to that intense erosion has been effected in the just outboard-side regions of the strike points. Except for that point, distribution of erosion on the outer target correlated with the frequency histogram of the strike point position. A sub-peak structure of the re-deposition layers found at around 50 mm on the inner target, on the other hand, cannot be reproduced well by the frequency histogram of the strike point position but by that after being weighted with total NBI power, $P_{\langle NB\rangle}$, for each shot (Fig. 7(c)). Re-deposition is likely to have been

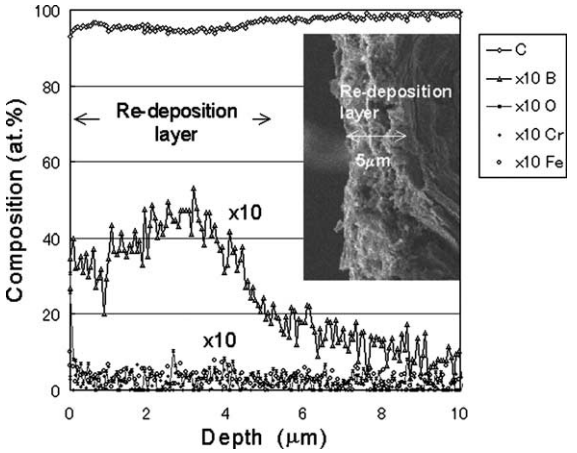

Fig. 4. Elemental depth profiles in re-deposition layer at mid zone on the inner divertor target of W-shaped divertor measured through XPS. An insertion is a cross-sectional SEM image of about 5-μm-thick re-deposition layer close to the XPS analysis point.

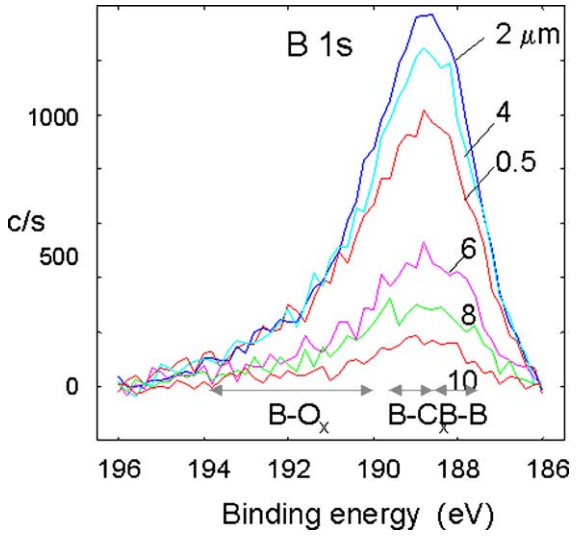

Fig. 5. B-1s photoelectron spectrum profiles at different depth in the re-deposition layer on the inner divertor target plate. Data from 0.4, 2.0 and 4.0 μm depths are assumed to be corresponding to those in the re-deposition layer.

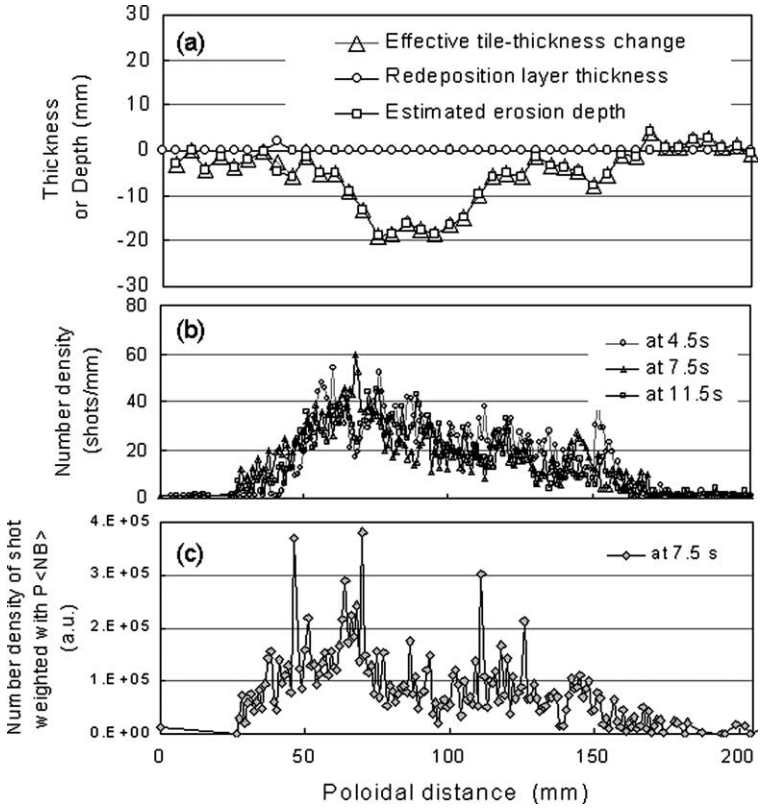

Fig. 6. Poloidal distribution of erosion depth on the outer divertor target (a), compared with that in frequency histogram of the strike point position (b) and that of the strike point position weighted with total NBI power $P_{(NB)}$ (c), for JT-60U in the June 1997–October 1998 experimental periods. Origin is at the inboard end of the outer target tile 5DV2cq.

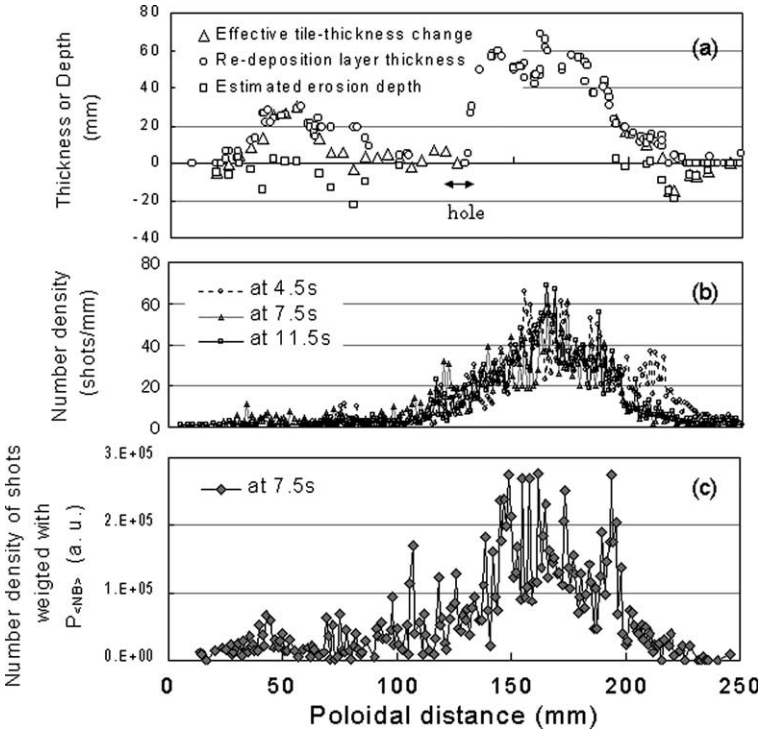

Fig. 7. Poloidal distribution of re-deposition layer thickness on the inner divertor target (a), compared with that in frequency histograms of the strike point position (b) and that of the strike point position weighed with total NBI power for each shots, $P_{\langle NB\rangle}$ (c), for JT-60U in the June 1997–October 1998 operation periods. Origin is at the inboard end and on the front face plane of the inner target tile 5DV2aq.

more enhanced in the higher NBI power experiments. Although re-deposition is dominant on the inner target, erosion was found partially in the 210–230 mm zone close to the slot, and both erosion and re-deposition were found locally on the inner 5DV2aq tile. Comparing Fig. 7(a) with Fig. 7(b) and (c), on the inner target, erosion is dominant either in the private flux regions in just outboard-side region of the separatrix or at the strike point in the start-up phase (Fig. 7(a) at 4.5 s) possibly due to the lower particle flux densities but the higher electron temperatures.

Plasma parameters namely electron temperature and electron density at the outboard strike point in L-mode cases are around 20 eV (more generally ranging in 15–50 eV [9] in the open divertor data) and around 4×10^{19} m^{-3}, respectively [7]. Maximum surface temperatures of the outer divertor target during shots are estimated to be in the 600–1200 K range [5]. Therefore, the observed erosion of the outer divertor targets is very probably due to chemical sputtering [10]. However, contributions of sputtering due to carbon impurity and high particle fluxes in ELM phases or other confinement modes in the operation periods have not been presently estimated.

Compared with the outer targets, the lower energies, therefore the lower heat fluxes were expected at the inner target. Those tendencies are supported by the lower temperatures measured for the inner target by means of thermo-couple elements embedded at 6 mm from the front faces in the relevant periods [5], as well as by the higher particle-recycling rates on the inboard side even in the inner-private flux pumping phase [8]. Thus on the inner divertor target, the re-deposition is dominant due to the lower plasma temperature leading to the lower erosion rate. Such in/out asymmetry in the erosion/re-deposition found in the present study, has been also reported for divertor regions of JET, DIII-D and ASDEX Upgrade [1,2]. In the future carbon-walled machines, lifetime of divertor targets will largely depend on controlling of the in/out asymmetry of erosion/re-deposition as well as on lowering of plasma temperatures at the targets. Tritium inventory in the re-deposition layer in the strike point zone on the targets may be substantially lowered due to the lower thermal conductivity of the re-deposition layers.

4. Conclusions

Graphite and CFC tiles used in the W-shaped divertor regions of JT-60U in D–D experimental periods, July 1997–October 1998, were investigated with respect

to erosion/re-deposition. Following conclusions were deduced:

(1) Asymmetries in erosion/re-deposition were found: erosion dominated at the outer target, while re-deposition dominated at the inner target. Also, no continuous re-deposition layers were found for the outer dome wing and the dome top, while continuous re-deposition layers were found on the inner dome wing at least in the zone close to the dome top, (2) the maximum erosion depth of around 20 μm was found on the outer target, while re-deposition layers of a maximum thickness around 60 μm were found on the inner target, (3) columnar structured layers with the thickness of less than 30 μm were found in the re-deposition layers. Lamellar structure layers were observed in the over-layers on the columnar layers, forming lamellar/columnar-layered structures with the total thickness of around 60 μm, (4) poloidal distribution of the erosion depth on the outer divertor target was correlated with those in the frequency histograms of separatrix strike point positions, and with that after weighting with total NBI power for each shot, (5) poloidal distribution of the re-deposition layer thickness on the inner target correlated well with that in the frequency histogram of the strike point positions after weighting with total NBI power for each shots, (6) atomic composition of the re-deposition layer in the mid zone of the inner target plate was C: 94–95, B: 3–4, O: 0.4–0.6, and Fe, Ni, Cr: 0.3–0.6 at.%. Boron atoms in the re-deposition layer on the inner target were concluded to be mainly in B–C, and possibly in B–B bonding.

For quantitative analyses in mass balance between erosion and re-deposition of divertor targets, estimation of average volumetric densities of the re-deposition layers will be indispensable. Those data are scarce now, and have to be measured in near future.

Acknowledgements

The present authors are grateful to members of JT-60U team for their valuable discussions and comments on the present study.

References

[1] D.G. Whyte, J.P. Coad, P. Franzen, H. Maier, Nucl. Fusion 39 (1999) 1025.
[2] G. Federici et al., Nucl. Fusion 41 (12R) (2001) 1967.
[3] A. Sagara, S. Masuzaki, T. Morisaki, et al., these Proceedings.
[4] Y. Hirohata, Y. Oya, H. Yoshida, et al., Proc. International Workshop on Hydrogen Isotopes in Fusion Reactor Materials, 22–24 May 2002, Tokyo, Japan;
Y. Oya, Y. Hirohata, et al., these Proceedings.
[5] K. Masaki, K. Sugiyama, et al., these Proceedings.
[6] T. Tanabe et al., these Proceedings.
[7] N. Asakura, N. Hosogane, K. Itami, et al., J. Nucl. Mater. 266–269 (1999) 182.
[8] N. Asakura, H. Tamai, et al., J. Nucl. Mater. 290 (2001) 825.
[9] H. Takenaga, H. Kubo, et al., Fusion Sci. Technol. 42 (2002) (JT-60 Special Issue) 327.
[10] S. Higashijima, H. Kubo, et al., J. Nucl. Mater. 266–269 (1999) 1078.